Research Square

Preprints are preliminary reports that have not undergone peer review.
They should not be considered conclusive, used to inform clinical practice,
or referenced by the media as validated information.

Bio-prospecting Seaweed-Associated Marine Bacteria for Polyhydroxyalkanoate Biosynthesis: Process Optimization and Biopolymer Characterization

Rubyga Nagarajan
Manonmaniam Sundaranar University
Uma Ganapathi
Manonmaniam Sundaranar University
Anusha John Radha
Manonmaniam Sundaranar University
Gharishma Roy Sakthivel Latha
Manonmaniam Sundaranar University
Citarasu Thavasimuthu
citarasu@gmail.com

Manonmaniam Sundaranar University

Research Article

Keywords: Bacillus thuringiensis, Marine bio-prospecting, Polyhydroxyalkanoate, Process optimization, Seaweed associated bacteria

Posted Date: November 27th, 2026

DOI: https://doi.org/10.21203/rs.3.rs-11797538/v1

License: This work is licensed under a Creative Commons Attribution 4.0 International License.
Read Full License

Additional Declarations: No competing interests reported.

Bio-prospecting Seaweed-Associated Marine Bacteria for Polyhydroxyalkanoate Biosynthesis: Process Optimization and Biopolymer Characterization

Rubyga Nagarajan[1] · Uma Ganapathi[1] · Anusha John Radha[1, 2] · Gharishma Roy Sakthivel Latha[1] · Citarasu Thavasimuthu[1*]

Abstract

Polyhydroxyalkanoates (PHAs) are biodegradable polyesters that many microorganisms accumulate as intracellular granules during fermentation. Bacteria associated with the seaweeds Ulva sp. and Sargassum sp. from the Arokiapuram shore (Kanyakumari District, Tamil Nadu, India) were isolated, screened for PHA production and identified. All twenty morphologically different isolates were tested with Sudan Black B and Nile Blue A stains. Sudan Black B stained twelve isolates positively, and four of them (U5, U9, S4 and S6) also fluoresced with Nile Blue A. Isolate S4 yielded the most PHA (13.6 g/L); morphological, biochemical and 16S rRNA sequence data identified it as *Bacillus thuringiensis* PHB CMST2 (GenBank accession OQ804398). In one-variable-at-a-time (OVAT) trials, glucose and ammonium chloride proved the most effective carbon and nitrogen sources, and PHA accumulation was highest at pH 6, 5% salinity and 35 °C. These variables (glucose, ammonium chloride and salinity) were then tuned with a central composite design within response surface methodology (RSM-CCD). Validation at the predicted optimum (1% glucose, 0.1% ammonium chloride, 5% salinity) gave 20 g/L PHA, close to the model prediction of 19.86 g/L (R^2 = 98.23%). The polymer was characterised as polyhydroxybutyrate by UV-visible spectroscopy, TLC and FT-IR (ester C=O stretch at 1724.24 cm^{-1}), together with thermogravimetry (complete degradation by 550 °C), XRD (amorphous), GC-MS and SEM-EDS (porous surface; C 55.6%, O 34.5%). These results suggest that the seaweed-associated *B. thuringiensis* PHB CMST2 is a promising, low-cost source of PHA from marine biomass.

Keywords *Bacillus thuringiensis* · Marine bio-prospecting · Polyhydroxyalkanoate· Process optimization· Seaweed associated bacteria

* Corresponding author Citarasu Thavasimuthu
citarasu@gmail.com

[1] Centre for Marine Science & Technology, Manonmaniam Sundaranar University, Rajakkamangalam, Kanyakumari District, Tamil Nadu, India
[2] Advanced Institute for Wildlife Conservation, Tamil Nadu Forest Department, Vandalur, Chennai - 600 048, Tamil Nadu, India.

Introduction

Plastic pollution is a growing environmental problem. Global plastic production reached about 460 million tonnes in 2019 [1], which shows how urgently sustainable alternatives are needed. Because petroleum-based plastics are chemically very stable, they resist breakdown and may remain in the environment for centuries or even millennia [2]. Each year an estimated 4.8–12.7 million metric tons of plastic debris reach the oceans [3], injuring wildlife [4], degrading ecosystems [5] and posing risks to human health [6]. The COVID-19 pandemic aggravated the problem through a steep rise in single-use plastics, personal protective equipment in particular [7]. Biodegradable and bio-based plastics have been developed in response to this problem.

Polyhydroxyalkanoates (PHAs) are among the biodegradable polymers regarded as promising replacements for certain conventional plastics. PHAs are completely biodegradable and have mechanical properties close to those of petroleum-derived polypropylene (PP) [8]. Microorganisms synthesise PHAs by fermentation, converting carbon substrates into a polymer that is stored as intracellular granules [9,10]. Reported PHA producers range from *Cupriavidus necator* [11] and *Bacillus* spp. [12] to *Pseudomonas* spp. [13] and engineered *Escherichia coli* [14].

PHA production still faces several challenges: it depends on pure carbon sources such as glucose, different PHA types need different organic co-substrates, contamination is a risk, and downstream processing uses large amounts of solvent [15]. Marine macroalgae, particularly green seaweeds such as *Ulva* sp., have emerged as promising renewable feedstocks for PHA because they are widely distributed, grow quickly, and are rich in carbohydrates. Unlike terrestrial crops, macroalgae need no arable land, freshwater irrigation, or heavy use of fertilizers and pesticides, so they compete less with food production and place fewer demands on agricultural resources [16, 17]. *Ulva* also contains substantial amounts of fermentable sugars, including glucose and rhamnose, which can support microbial growth and PHA synthesis after suitable pretreatment or hydrolysis [18,19].

The surface and internal tissues of seaweeds are nutrient-rich niches that support diverse bacterial communities able to use algal exudates and complex organic compounds. These seaweed-associated bacteria are therefore a valuable source of new PHA producers with potentially useful metabolic and physiological traits. Gnaim et al. [19] recovered PHA-producing *Cobetia, Bacillus, Pseudoalteromonas* and *Sulfitobacter* from *Ulva* sp. Similarly, Ghosh et al. [18] found *Ulva* hydrolysate to be a suitable PHA feedstock. Together, these findings show that seaweed biomass can be turned into value-added biodegradable polymers.

Using naturally occurring or waste seaweed biomass for PHA production could also support a circular bioeconomy by turning underused marine biomass into biodegradable, commercially valuable polymers, and it offers an alternative to petroleum-derived plastics. Macroalgal biomass has already been converted into other bio-based products such as biofuels and biochemicals, which points to its wider potential as a biorefinery feedstock [19, 20]. The present work therefore isolates and identifies PHA-producing bacteria from seaweeds collected from the Arokiapuram coast (Kanyakumari District) and optimizes PHA production by the selected strain. The polymer was then characterized by TLC, FT-IR, GC-MS, and other techniques.

Materials and Methods

Collection of samples and isolation of seaweed-associated bacteria

Ulva sp. and *Sargassum* sp. were collected from the Arokiapuram coast (8.11899° N, 77.5577° E), Kanyakumari District, sealed in sterile plastic bags, and brought to the laboratory at 4 °C. The samples were rinsed thoroughly in sterile seawater to remove sand, debris, and loosely attached organisms. One gram of tissue was ground with a sterile mortar and pestle in 9 mL of sterile saline. The homogenate was diluted in a ten-fold series, and 0.1 mL of suitable dilutions was plated in triplicate on Zobell Marine Agar (ZMA). Plates were kept at 28 °C for 24 h. Colonies that differed in colour, shape, elevation or margin were picked and purified by repeated streaking on fresh ZMA; the pure isolates were maintained as 20% glycerol stocks at −80 °C [21].

Screening of PHA-producing bacterial isolates

For PHA screening, isolates were inoculated onto ZMA plates supplemented with 1% glucose as a carbon-rich medium. After 24 h of growth, the plates were covered with 0.02% Sudan Black B in alcohol and left standing for 20 min. The surplus amount of stain was

drained, and the plates were washed with absolute alcohol. Colonies that produced PHA appeared bluish-black. Sudan Black B-positive isolates were re-tested by the viable-colony method with Nile Blue A by streaking on ZMA containing 1% glucose and 0.5 µg/mL Nile Blue A. Under UV light, PHA-containing colonies glowed bright orange, and the glow intensified as intracellular PHA increased. The isolates showing bright orange fluorescence were selected as PHA accumulators [22, 23].

Extraction of accumulated PHA by the modified hypochlorite method

The isolates that were positive in the Nile Blue A assay were then quantified for PHA accumulation. The positive isolates were cultured in sterile Zobell marine broth with 1% glucose at 30 °C for 48 h, and PHA was recovered by the modified hypochlorite method of Rawte and Mavinkurve [24]. Cells were harvested by centrifugation (8,500 rpm, 15 min). The supernatant was discarded and the pellet was rinsed in distilled water and spun again (7,500 rpm, 15 min). The washed pellet was air-dried for 2 h and weighed to give the dry cell weight. The dried cells were re-suspended in 5 mL of 2% sodium hypochlorite, vortexed and held at 37 °C for 30 min. The PHA was pelleted (6,500 rpm, 10 min), washed with acetone: alcohol (1:1 v/v), vortexed and dissolved in 5 mL chloroform. The chloroform solution was transferred to a glass Petri dish and left to evaporate at 28 °C. The PHA powder was weighed after evaporation [25].

Residual biomass (g/l) = Dry Cell Weight (g/l) - Dry weight of extracted PHAs (g/l)

$$\text{PHA accumulation (\%)} = \frac{Dry\ weight\ of\ extracted\ PHA\ (\frac{g}{L})}{Dry\ Cell\ Weight\ (DCW)(\frac{g}{L})}\ \text{x}\ 100$$

Morphological and molecular identification of the selected PHA-producing bacterial isolate

The colony and biochemical traits of the best PHA producer were examined following Bergey's Manual of Systematic Bacteriology [26]. Genomic DNA was extracted by the phenol–chloroform method [27]. The 16S rRNA gene was amplified by PCR with the universal primers 27F (AGAGTTTGATCMTGGCTCAG) and 1492R (TACGGYTACCTTGTTACGACTT) [28] and sequenced. Sequence similarity was searched with BLAST [29], and the phylogenetic tree was constructed in MEGA 6.0 [30].

Optimization of culture media for PHA production

One-factor-at-a-time (OFAT) optimization

The effects of incubation time (1, 2, 3, and 4 days), pH (5 to 9), temperature (25, 30, 35, 37, and 40°C), and salinity (2, 3, 4, and 5%) on PHA production and accumulation were tested.

Carbon sources (glucose, fructose, sucrose, maltose, dextrose and lactose; 2% each) and nitrogen sources (ammonium sulfate, peptone, yeast extract, potassium nitrate, ammonium chloride and urea; 0.2% each) were compared in mineral salt media prepared according to Kumar et al. [31] and Muigano et al. [32].

Optimization of culture media for PHA production using Response Surface Methodology–Central Composite Design (RSM-CCD)

The media was optimised by Response Surface Methodology with a Central Composite Design (RSM-CCD). Statistical experimental design reduces the number of runs, time and materials needed to learn how process variables influence a response, which is why it is so widely used. The three variables that the OVAT trials had shown to matter, glucose (A), ammonium chloride (B) and salinity (C), were then optimised using a central composite design (CCD). Using MINITAB 19 with three factors at five levels, a design of 20 experiments was generated. Each variable was set at five coded levels ($-\alpha$, -1, 0, $+1$, $+\alpha$), with 0 as the centre point and α as the axial (star) distance.

A second-order polynomial regression model was fitted to the coded values according to the RSM (CCD) design [33, 34]:

$$Y = \beta_0 + \beta_1 A + \beta_2 B + \beta_3 C + \beta_{11} A^2 + \beta_{22} B^2 + \beta_{33} C^2 + \beta_{12} AB + \beta_{13} AC + \beta_{23} BC$$

where Y is the predicted PHA yield, β_0 the intercept, A, B and C the coded levels of glucose, ammonium chloride and salinity, β_1–β_3 the linear, β_{11}–β_{33} the quadratic and β_{12}, β_{13}, β_{23} the interaction coefficients.

Preparation of PHA films

For film casting, 50 mg of PHA was dissolved in 1 mL chloroform and heated in an oven at 50 °C until the solvent had evaporated, leaving a PHA film [35].

Characterization of PHA

PHA granules were released by digesting cells with alkaline sodium hypochlorite and collected by centrifugation. The granules were precipitated and treated with concentrated sulfuric acid, which converts PHA to crotonic acid. PHA was detected through its conversion to crotonic acid, measured by absorbance at 220–240 nm in a UV spectrophotometer [36, 37]. For TLC, the PHA film was redissolved in chloroform and a drop of the solution was applied to a silica gel plate. The plate was developed for 40 min in chloroform–methanol (1:1) and then exposed to iodine vapour for 5–10 min in a chamber set over a water bath [38, 39]. The extracted PHA was analyzed by FT-IR spectroscopy using a Shimadzu instrument and the spectra were recorded over 4000–500 cm^{-1} [40].

The polymer composition was analyzed by GC–MS. For GC-MS, dried cells were methanolysed in a mixture of 2 mL chloroform, 0.3 mL concentrated (98%) sulfuric acid and 1.7 mL methanol at 100 °C for 140 min, converting the monomers to methyl esters. The mixture was cooled to room temperature, 1 mL water was added to separate the layers, and the lower chloroform phase was analysed by GC-MS [41, 42]. TG–DTA was performed on a thermal analyzer (EXSTAR: SIINT 6300) following Lorini et al. [43]. About 20 mg of dried sample was heated from 30 to 800 °C at 10 °C/min under flowing air (50 mL/min) while weight loss and heat flow were recorded.

XRD analysis was carried out on a Bruker D2 Phaser with CuKα radiation [44, 45]. XRD patterns were recorded at room temperature (40 kV, 10 mA) over a 2θ range of 10–80°. The d-spacing was obtained from Bragg's law, and the crystallinity index from the ratio of crystalline peak area to total scattered area.

SEM was used to examine the surface morphology and elemental composition of the PHA films. Films were fixed on stubs with carbon tape and viewed in a Carl Zeiss EVO18 instrument [46].

Results

Isolation and Screening of PHA-Producing Bacteria

Serial dilution of the seaweed samples gave twenty morphologically different bacterial isolates. Twelve of them took up Sudan Black B and appeared bluish-black (Fig. 1), indicating PHA granules. Nile Blue-A staining then confirmed four of these strains (U5, U9, S4, and S6) as PHA producers (Fig. 2), and these were selected for further study.

PHA Extraction and Quantification

PHA was extracted from all four selected strains to compare their production. Strain S4 gave the highest yield, 13.6 g/L, ahead of all the other isolates (Table 1), so it was chosen for morphological, biochemical, and molecular identification.

Morphological and Molecular Identification of the PHA-producing bacterial strain S4

Strain S4 was a Gram-positive rod. BLAST analysis of the 16S rRNA gene sequence showed 100% identity with *Bacillus thuringiensis* (MK875245.1) (Fig. 3), and the isolate was designated *Bacillus thuringiensis* PHB CMST2. The sequence is deposited in GenBank under accession number OQ804398.

One-Factor-at-a-Time Optimization of Culture Conditions

In the OFAT experiments, glucose gave the highest PHA yield among the carbon sources (8.6 g/L; Table 2) and ammonium chloride among the nitrogen sources (7 g/L; Table 3). The highest yield was reached after 2 days of incubation (3.2 g/L; Table 4). Among the pH values tested, pH 6 was optimal (11.2 g/L; Table 5), 5% NaCl was the best salinity (9 g/L; Table 6), and 35°C was the best temperature, although the yield was comparatively low (4 g/L; Table 7).

RSM-CCD Optimization of PHA Production by *Bacillus thuringiensis* PHB CMST2

Twenty runs of a central composite design (CCD) within RSM were carried out to assess the joint effects of glucose (A), ammonium chloride (B) and salinity (C) on PHA production by *Bacillus thuringiensis* PHB CMST2 (Table 8). Dry PHA weight ranged from 0.11 g/L (Run 20; 3% glucose, 0.3% ammonium chloride, 1% salinity) to 11.55 g/L (Run 4; 3% glucose, 0.1% ammonium chloride, 3% salinity), the highest yield within the design matrix.

The second-order polynomial equation for dry PHA weight (g/L) in un-coded units was:

Dry PHA weight (g/l) = 15.77 + 0.413 (Glucose) − 98.83 (Ammonium chloride) + 0.876 (Salinity) + 0.108 (Glucose)² + 145.4 (Ammonium chloride)² + 0.461 (Salinity)² − 0.22 (Glucose × Ammonium chloride) − 0.510 (Glucose × Salinity) − 2.68 (Ammonium chloride × Salinity)

ANOVA showed the model to be highly significant ($F = 61.52$, $p < 0.001$), so the quadratic equation describes how the variables affect PHA production well (Table 9). Ammonium chloride had significant linear ($F = 118.83$, $p < 0.001$) and quadratic ($F = 179.79$, $p < 0.001$) effects, making nitrogen concentration the dominant factor controlling PHA yield. The quadratic term for salinity ($F = 18.10$, $p = 0.002$) and the glucose × salinity interaction ($F = 12.28$, $p = 0.006$) were also significant. The linear effects of glucose ($p = 0.659$) and salinity ($p = 0.357$) and the interactions glucose × ammonium chloride ($p = 0.882$) and ammonium chloride × salinity ($p = 0.096$) was not significant. A non-significant lack of fit ($F = 3.16$, $p = 0.116$) shows that the model fits the data adequately.

The model explained most of the variation ($R^2 = 98.23\%$), with an adjusted R^2 of 96.63% and a predicted R^2 of 89.17%, so predicted and experimental values agree closely (Table 10). One observation (Run 18) had a relatively large standardized residual (2.29) but was not considered to affect the overall fit.

The regression equation for Dry PHA (gm/L) = 15.77+ 0.413 Glucose (%) - 98.83 Ammonium chloride (%) + 0.876 Salinity (%) + 0.108 Glucose (%)*Glucose (%)+ 14 5.4 Ammonium chloride (%)*Ammonium chloride (%)+ 0.461 Salinity (%)*Salinity (%)-

0.22 Glucose (%)*Ammonium chloride (%)- 0.510 Glucose (%)*Salinity (%) - 2.68 Ammonium chloride (%)*Salinity (%)

Fig. 4 presents three-dimensional response surfaces and contour plots of the effect of glucose, ammonium chloride, and salinity on PHA production; they show that PHA yield varies non-linearly with nitrogen and salinity. Numerical optimization of the fitted model for maximum dry PHA weight predicted an optimum of 1% glucose, 0.1% ammonium chloride, and 5% salinity, giving a predicted PHA concentration of 19.86 g/L (95% CI: 17.01–22.71 g/L; composite desirability = 1.0) (Fig. 5; Table 11).

PHA Film Preparation

A biofilm was cast from the PHA extracted from *Bacillus thuringiensis* PHB CMST2 (Fig. 6).

Characterization of the Extracted PHA

UV-visible analysis gave an absorption maximum at 230–240 nm, confirming PHA (Fig. 7). TLC also confirmed PHA: after the plate was placed in the iodine chamber, yellowish-green spots appeared (Fig. 8), with an Rf value of 0.769.

The FT-IR spectrum of the extracted polymer showed bands typical of PHA (Fig. 9). The strong, sharp band at 1724.24 cm^{-1} corresponds to the ester carbonyl (C=O) stretch, the principal marker of the PHA polyester backbone. Bands at 2972.10, 2879.52 and 2825.52 cm^{-1} arise from asymmetric and symmetric C–H stretching of CH_3 and CH_2 groups, in line with the aliphatic side chains of PHA monomers. The broad absorption near 3291.30 cm^{-1} (with weaker bands at 3724.29 and 3607.60 cm^{-1}) indicates O–H stretching, probably from residual hydroxyl groups or moisture. C–H bending of CH_3 and CH_2 groups accounts for the bands at 1452.30 and 1380.94 cm^{-1}. In addition, medium-to-strong bands at 1277.75, 1227.61, 1186.14, and 1134.07 cm^{-1} correspond to C–O–C stretching of the ester linkage, supporting the polyester nature of the polymer, while the intense band at 1055.95 cm^{-1} is due to C–O stretching of ester groups. The weaker bands at 978.81, 824.51, 687.58, 643.22, 546.78, 518.82, and 468.67 cm^{-1} correspond to C–C skeletal vibrations and out-of-plane bending, typical of the PHA backbone (Table 12). Together, the ester carbonyl band, the C–H stretching bands, and the C–O–C ester bands identify the polymer of *Bacillus thuringiensis* PHB CMST2 as a PHA.

GC-MS analysis of the acid-methanolyzed extract from *Bacillus thuringiensis* PHB CMST2 resolved 194 peaks in the total ion chromatogram (TIC) between 3.6 and 27.0 min (Fig. 10). The PHA was identified from the dimer of γ-hydroxybutyric acid, crotyl ester, and γ-hydroxy-methyl butyrate, at retention times of 22.688 min (Peak 143, 0.64% peak area) and

26.679 min (Peak 191, 0.16% peak area). These are diagnostic breakdown products of the poly(3-hydroxybutyrate) (PHB) backbone under acidic methanolysis and agree with the FT-IR ester carbonyl band at 1724.24 cm^{-1}.

Besides the PHA-derived monomer esters, the chromatogram was dominated by co-extracted fatty acid methyl esters (FAMEs) from residual cellular lipids, which is typical of bacterial biomass extracts. The most abundant were n-hexadecanoic acid (palmitic acid) at 20.596 min (7.73% peak area), hexadecanoic acid methyl ester at 20.219 min (5.87%), and 9-octadecenoic acid (Z)-methyl ester (methyl oleate), which appeared at several retention times (20.021, 21.145, 23.104, and 25.643 min) and together accounted for about 11% of the total peak area. Octadecanoic acid methyl ester (methyl stearate) was also detected at 22.240 min (0.77%). Minor peaks for short-chain fatty acid esters, including dodecanoic acid (16.001 min, 0.37%) and tetradecanoic acid, 12-methyl-, methyl ester (18.720 min, 0.10%), were also detected, along with many unidentified or trace volatile compounds, consistent with minor cellular metabolites and residual reagents from extraction and derivatization (Table 13).

TGA recorded a complete (100%) mass loss at 550 °C in three steps: 20% below 250 °C (bound water and volatiles), 40% up to 475 °C (breakdown of PHA chains), and the remaining 40% up to 550 °C (burning of residual organic matter) (Fig. 11). DTA showed a sharp exothermic peak at 520 °C, reflecting the heat released in the final combustion stage. These results describe the thermal stability and degradation behaviour of the PHB produced by *Bacillus thuringiensis* PHB CMST2.

XRD showed a broad peak at 23° and no sharp peaks (Fig. 12), indicating a mostly amorphous structure without long-range atomic order.

SEM analysis of the PHA produced by *Bacillus thuringiensis* strain PHB CMST2 was done at magnifications from 250× to 10,000× (EHT = 20 kV, WD = 10 mm, secondary electron mode). At low magnification (250× to 500×), the sample appeared as a continuous, dark, relatively smooth matrix with fine bright particles spread evenly over the whole field, along with a few larger radial clusters and fibrillar bundles. At 1,000× to 2,500× these particles resolved into small, star-shaped, branched aggregates of roughly 2–5 μm without large empty patches, and at 4,000× to 5,000× they showed rough, spiky surfaces with thin fibrillar arms radiating from a central point, giving a dendritic appearance. At 10,000×, the aggregates appeared as irregular, thin, flake-like and curled lamellar structures joined to the matrix by fine fibrils, and no smooth, uniformly spherical granules were observed. Overall, the polymer showed a rough, semi-crystalline texture with irregular, dendritic and fibrillar aggregates embedded in a continuous matrix (Fig. 13). EDS gave the following elemental

composition (wt%): carbon 55.6%, oxygen 34.5%, sodium 4%, magnesium 1.1%, phosphorus 2.8%, sulfur 1.3%, and chlorine 0.7%. Elemental mapping showed all of these elements spread throughout the sample (Fig. 14; Table 14).

Discussion

Marine biomass, and seaweed in particular, has attracted considerable attention as a renewable resource for biopolymer production. Seaweeds are abundant, inexpensive, and rich in carbohydrates, which makes them attractive substrates for microbial fermentation. Seaweed biomass is increasingly converted into products such as biofuels and biopolymers, and its use as a PHA substrate has been explored more and more in recent years [19]. With this in mind, we isolated seaweed-associated bacteria and assessed their capacity to produce PHA.

Seaweed-associated isolates were screened for PHA using Sudan Black B staining followed by Nile Blue A. Sudan Black B, one of the oldest stains for lipids, revealed intracellular lipophilic granules in several isolates, as in earlier studies [23, 47]. Nile Blue A confirmed PHA accumulation by bright orange fluorescence under UV light and is considered the more specific and sensitive stain for PHA [48]. Four isolates (U5, U9, S4, and S6) fluoresced strongly, indicating efficient PHA accumulation and showing that the screening methods worked.

Of the four PHA-positive isolates, strain S4 gave the highest yield (13.6 g/L) and was chosen for further work. Morphological and molecular analysis identified the strain as *Bacillus thuringiensis* PHB CMST2, whose 16S rRNA gene sequence was identical to that of a reference *B. thuringiensis* strain. Phylogenetic analysis placed it close to known *B. thuringiensis* strains, in line with earlier reports of PHA production in this genus [49-51]. *Bacillus* species are widely used in industry because they grow quickly, have low nutrient requirements, and can use many carbon sources. As Gram-positive bacteria, they also lack lipopolysaccharides (LPS), which is an advantage for large-scale PHA production [52].

PHA was extracted with the modified sodium hypochlorite method, which is widely used because it digests non-PHA cellular material efficiently while leaving the polymer granules intact [24, 25]. It gave purified PHA that was suitable for characterization.

Culture conditions had a strong effect on PHA production. The influence of carbon and nitrogen source, pH, temperature, salinity and incubation time was examined one factor at a time (OFAT). Glucose was the best carbon source, yielding 8.6 g/L PHA. This is

consistent with reports that Bacillus species differ in the substrates they prefer for PHA synthesis [53, 54]. Carbon sources serve both as an energy supply and as precursors for PHA biosynthesis.

Ammonium chloride was the best nitrogen source (7 g/L). Nitrogen limitation is well known to trigger PHA accumulation, because under nutrient stress bacteria shift their metabolism from growth to storage [55]. Restricted nitrogen supply has also boosted PHA synthesis in other bacterial strains [56].

Temperature and pH also affected PHA production. PHA accumulation peaked at pH 6, in line with the preference of many bacteria for neutral pH, where enzyme activity and metabolic efficiency are highest during PHA biosynthesis [57]; even small departures from the optimum can lower enzyme activity and polymer yield considerably. The optimal temperature was 35°C, the same as reported by Sachan et al. [58] for *Bacillus paranthracis* RSKS-3 in an RSM study. In our study, PHA accumulation peaked after 2 days (48 h) of incubation. Ibrahim et al. [59] found a later peak, at 96 h, in *Bacillus licheniformis* AZU-A5; differences in strain, growth rate, and cultivation conditions could explain the difference.

RSM-CCD is an efficient statistical tool for optimizing several interacting variables in fermentation while keeping the number of runs low [60]. We used it to optimize glucose, ammonium chloride, and salinity for PHA production by *Bacillus thuringiensis* PHB CMST2, after these were identified as important variables in the preliminary OVAT experiments. The second-order polynomial is the usual quadratic model in optimisation of fermentation and metabolite production [34]. The model was highly significant ($F = 61.52$, $p < 0.001$) and its lack of fit was not significant ($p = 0.116$), so the quadratic equation adequately explains how the variables affect PHA yield. The R^2 of 98.23%, and the close agreement between adjusted R^2 (96.63%) and predicted R^2 (89.17%), indicate a robust, predictive model, in line with the criteria suggested for well-fitting RSM models in bioprocess optimization [60].

Ammonium chloride influenced PHA production most strongly, with highly significant linear and quadratic terms (both $p < 0.001$), indicating that nitrogen supply was the main determinant of polymer accumulation in this isolate. This fits the established principle that bacteria make PHA when nutrients, especially nitrogen, are limited, and carbon is diverted from growth to intracellular storage [55, 56]. The significant quadratic effect of salinity and its significant interaction with glucose suggest that osmotic stress and carbon availability act together on PHA accumulation in this seaweed-associated isolate, which would be a plausible adaptation to its marine origin.

Numerical optimisation predicted a maximum yield of 19.86 g/L at 1% glucose, 0.1% ammonium chloride and 5% salinity (composite desirability = 1.0). Experimental validation under these conditions gave 20 g/L PHA, very close to the prediction, which supports the accuracy of the RSM-CCD approach for this isolate. The validated yield is well above both the best run in the original CCD matrix (11.55 g/L) and the yield from single-factor optimization with glucose alone (8.6 g/L), showing the benefit of multivariate optimization over testing one factor at a time. RSM-based optimization has produced similar gains in other *Bacillus* systems; for example, RSM optimization of *Bacillus paranthracis* RSKS-3 raised PHA production several-fold [60].

The absorption peak at 230–240 nm in the UV–Visible spectrum confirms PHA, because sulfuric acid treatment converts the polymer to crotonic acid. The crotonic acid assay was first described by Law and Slepecky [36], and Sachan et al. [58] likewise reported an absorption peak near 235 nm for crotonic acid formed from PHA by acid treatment. The result supports the crotonic acid assay as a reliable method for detecting and quantifying PHA.

On the TLC plate, the extracted polymer gave one yellowish-green spot after iodine staining (Rf = 0.769), close to the Rf of about 0.8 reported for PHB by Semeniuk et al. [61].

The FT-IR spectrum showed a strong ester C=O stretch at 1724.24 cm^{-1}, with C–H stretching (2972.10, 2879.52 cm^{-1}), C–H bending (1452.30, 1380.94 cm^{-1}) and C–O–C ester bands (1277.75–1055.95 cm^{-1}), which are characteristic of polyhydroxybutyrate (PHB). The minor bands at 1661.56 and 1547.77 cm^{-1}, tentatively assigned to residual amide groups, point to trace protein contamination that did not prevent identification of the PHA. Similar spectra were reported by Gedikli et al. [62] and Stanley et al. [63].

TG-DTA showed that the extracted PHA degraded completely by 550°C, in three stages: loss of moisture and volatile compounds (up to 250°C), degradation of the PHA chains (up to 475°C), and final combustion of the remaining organic material (up to 550°C). The DTA curve had an exothermic peak at 520°C, reflecting the large release of heat during final combustion. Lorini et al. [43] and Sachan et al. [58] observed comparable thermal behaviour for bacterial PHA.

XRD showed a broad peak at about 23° (2θ) and no sharp peaks, indicating a mostly amorphous structure. This agrees with Sedláček et al. [64], who reported that PHA stored inside bacterial cells is mainly amorphous. The low crystallinity we observed may therefore reflect the native, intracellular granular state of the polymer.

GC-MS of the methanolyzed extract confirmed the identity of the polymer through the characteristic methanolysis products, the dimer of γ-hydroxybutyric acid, crotyl ester and γ-hydroxy-methyl butyrate, at 22.688 and 26.679 min, which is the diagnostic pattern for poly(3-hydroxybutyrate) under acidic methanolysis. The chromatogram also contained several co-extracted fatty acid methyl esters, mainly palmitic acid (n-hexadecanoic acid), methyl palmitate, methyl oleate, and methyl stearate, which together made up a substantial part of the total peak area. These most likely come from cellular lipids co-extracted with the polymer rather than from PHA monomers, and fatty acid interference has been reported in GC-MS analysis of crude bacterial PHA extracts [65]. The largest single peak, tentatively identified as dibutyl phthalate (15.14% peak area), is probably a background artifact: phthalate esters are common plasticizer contaminants from laboratory plasticware and solvents, not microbial metabolites.

The morphology observed in SEM differs from that of native PHA granules, which are generally described as smooth, spherical inclusions of 0.2–0.5 μm, surrounded by phospholipids and granule-associated proteins and held in a mobile, largely amorphous state inside the cell [66, 67]. Once PHA is extracted and the granule membrane is removed, the polymer chains can crystallize, and the final morphology depends strongly on how the polymer is recovered and cast [68, 69]. Rapid precipitation or solvent evaporation gives rough, heterogeneous surfaces, because crystal nuclei form quickly and grow outward as radial, fibrillar or dendritic structures [68, 70]. The star-shaped and fibrillar aggregates seen here are consistent with this, so the rough, semi-crystalline appearance most likely reflects solvent-induced crystallisation after extraction, not the native granule shape. Similar irregular surface morphologies have been reported for PHAs from other *Bacillus* species [71, 72], and such a microstructure can influence mechanical behaviour and degradation rate, since crystalline regions are degraded by depolymerases more slowly than amorphous ones [8, 73]. Because SEM gives only surface morphology, the degree of crystallinity should be confirmed by XRD, DSC and FTIR analysis [74, 75]. EDS showed that carbon (55.6%) and oxygen (34.5%) dominate, as expected for a polyester such as PHA. The minor elements (sodium, magnesium, phosphorus, sulfur, and chlorine) probably come from residual salts in the culture medium or extraction buffers rather than from the polymer itself. Similar porous morphology and carbon- and oxygen-dominated composition have been reported for bacterial PHA [58].

Overall, our results show that the seaweed-associated *Bacillus thuringiensis* PHB CMST2 is a promising candidate for PHA production. Optimizing the culture conditions

raised polymer yield, which speaks to one of the main obstacles to commercial PHA, its high production cost. Using marine biomass and its associated microbes as a source also adds to the sustainability of the process. However, the yields from the OFAT experiments and the RSM runs differ in scale, so the size of the improvement from statistical optimization should be interpreted with caution.

Conclusions

In conclusion, this study shows that seaweed-associated marine bacteria, specifically *Bacillus thuringiensis* PHB CMST2, have potential for PHA production. UV-Vis spectroscopy, TLC, FT-IR, TG-DTA, XRD, GC-MS, and SEM-EDS together confirmed that the isolate produces polyhydroxybutyrate (PHB) with an amorphous, thermally stable, porous structure. The screening and extraction protocols worked well for isolating and confirming PHA producers from a little-explored marine niche. Future work should scale up production, refine downstream purification to reduce co-extracted lipids and plasticizer contamination in the analytical data, and evaluate the mechanical properties of the polymer to assess its suitability for industrial use.

Acknowledgements The author T. Citarasu gratefully acknowledges the University Grants Commission (UGC), New Delhi, Government of India, for its financial support, in the form Special Assistance Programme (SAP) [UGC NO. F.3-24/2012 (SAP-II) dated October 2012].

Author contributions R.N and G.R.S.L are involved the entire experimental works. UG and A.J.R involved writing – original draft, data curation, methodology and editing. T.C – Conceptualization, review & editing

Data Availability Data will be made available on request.

Declarations

Conflict of interest The authors declare no conflict of interest.

References

1. OECD (2022). Global plastics outlook: Economic drivers, environmental impacts and policy options. OECD Publishing. https://doi.org/10.1787/de747aef-en
2. Barnes DKA, Galgani F, Thompson RC, Barlaz M (2009). Accumulation and fragmentation of plastic debris in global environments. Philosophical Transactions of

the Royal Society B: Biological Sciences 364(1526): 1985–1998. https://doi.org/10.1098/rstb.2008.0205

3. Jambeck JR, Geyer R, Wilcox C, Siegler TR, Perryman M, Andrady A, Narayan R, Law KL (2015) Plastic waste inputs from land into the ocean. Science 347(6223): 768–771. https://doi.org/10.1126/science.1260352
4. Marn N, Jusup M, Kooijman SALM, Klanjscek T (2020) Quantifying impacts of plastic debris on marine wildlife identifies ecological breakpoints. Ecology Letters 23(10): 1479–1487. https://doi.org/10.1111/ele.13574
5. Lamb JB, Willis BL, Fiorenza EA, Couch CS, Howard R, Rader DN, True JD, Kelly LA, Ahmad A, Jompa J, Harvell CD (2018) Plastic waste associated with disease on coral reefs. Science 359(6374): 460–462. https://doi.org/10.1126/science.aar3320
6. Thompson RC, Moore CJ, vom Saal FS, Swan SH (2009) Plastics, the environment and human health: Current consensus and future trends. Philosophical Transactions of the Royal Society B: Biological Sciences 364(1526): 2153–2166. https://doi.org/10.1098/rstb.2009.0053
7. Silva ALP, Prata JC, Walker TR, Duarte AC, Ouyang W, Barceló D, Rocha-Santos T (2021) Increased plastic pollution due to COVID-19 pandemic: Challenges and recommendations. Chemical Engineering Journal 405: 126683. https://doi.org/10.1016/j.cej.2020.126683
8. Khanna S, Srivastava AK (2005) Recent advances in microbial polyhydroxyalkanoates. Process Biochemistry 40(2): 607–619. https://doi.org/10.1016/j.procbio.2004.01.053
9. Yu L, Dean K, Li L (2006) Polymer blends and composites from renewable resources. Progress in Polymer Science, 31(6): 576–602. https://doi.org/10.1016/j.progpolymsci.2006.03.002
10. Mathuriya AS, Yakhmi JV, Martínez LMT, Kharissova OV, & Kharisov BI (2017) Polyhydroxyalkanoates: Biodegradable plastics and their applications. In Handbook of Ecomaterials. Springer, pp 1029. https://doi.org/10.1007/978-3-319-48281-1_84-1
11. Sohn YJ, Son J, Jo SY, Park SY, Yoo JI, Baritugo KA, Na JG, Choi JI, Kim HT, Joo JC, Park SJ (2021) Chemoautotroph *Cupriavidus necator* as a potential game-changer for global warming and plastic waste problem: A review. Bioresource Technology 340: 125693. https://doi.org/10.1016/j.biortech.2021.125693
12. Mohapatra S, Mohanta PR, Sarkar B, Daware A, Kumar C, Samantaray DP (2017) Production of polyhydroxyalkanoates (PHAs) by *Bacillus* strain isolated from waste

water and its biochemical characterization. Proceedings of the National Academy of Sciences, India Section B: Biological Sciences 87: 459–466. https://doi.org/10.1007/s40011-015-0626-6

13. Mozejko-Ciesielska J, Szacherska K, Marciniak P (2019) *Pseudomonas* species as producers of eco-friendly polyhydroxyalkanoates. Journal of Polymers and the Environment 27: 1151–1166. https://doi.org/10.1007/s10924-019-01422-1
14. Leong YK, Show PL, Ooi CW, Ling TC, Lan JCW (2014) Current trends in polyhydroxyalkanoates (PHAs) biosynthesis: Insights from the recombinant Escherichia coli. Journal of Biotechnology 180 52–65. https://doi.org/10.1016/j.jbiotec.2014.03.020
15. Rodriguez-Perez S, Serrano A, Pantión AA, Alonso-Farinas B (2018) Challenges of scaling-up PHA production from waste streams. A review. Journal of Environmental Management 205: 215–230. https://doi.org/10.1016/j.jenvman.2017.09.083
16. Wei N, Quarterman J, Jin YS (2013) Marine macroalgae: An untapped resource for producing fuels and chemicals. Trends in Biotechnology 31(2): 70–77.
17. Gajaria TK, Suthar P, Baghel RS, Balar NB, Sharnagat P, Mantri VA, Reddy CRK (2017) Integration of protein extraction with a stream of byproducts from marine macroalgae: A model forms the basis for marine bioeconomy. Bioresource Technology 243: 867–873. https://doi.org/10.1016/j.biortech.2017.06.149
18. Ghosh S, Gnaim R, Greiserman S, Fadeev L, Gozin M, Golberg A (2019) Macroalgal biomass subcritical hydrolysates for the production of polyhydroxyalkanoate (PHA) by *Haloferax mediterranei*. Bioresource Technology, 271: 166–173. https://doi.org/10.1016/j.biortech.2018.09.108
19. Gnaim R, Polikovsky M, Unis R, Sheviryov J, Gozin M, Golberg A (2021) Marine bacteria associated with the green seaweed *Ulva* sp. for the production of polyhydroxyalkanoates. Bioresource Technology 328: 124815. https://doi.org/10.1016/j.biortech.2021.124815
20. Ashokkumar V, Salim MR, Salam Z, Sivakumar P, Chong CT, Elumalai S, Suresh V, Ani FN (2017) Production of liquid biofuels (biodiesel and bioethanol) from brown marine macroalgae *Padina tetrastromatica*. Energy Conversion and Management, 135: 351–361. https://doi.org/10.1016/j.enconman.2016.12.054
21. Sinimol S, Sarika A R, Jayakumaran Nair A (2015) Diversity and antagonistic potential of marine microbes collected from south-west coast of India. 3 Biotech 6(1): 7. https://doi.org/10.1007/s13205-015-0318-1

22. Spiekermann P, Rehm BHA, Kalscheuer R, Baumeister D, Steinbuchel A (1999) A sensitive, viable-colony staining method using Nile red for direct screening of bacteria that accumulate polyhydroxyalkanoic acids and other lipid storage compounds. Archives of Microbiology 171(2): 73–80. https://doi.org/10.1007/s002030050681
23. Shah S, Kumar A (2021) Production and characterization of polyhydroxyalkanoates from industrial waste using soil bacterial isolates. Brazilian Journal of Microbiology 52: 715–726. https://doi.org/10.1007/s42770-021-00452-z
24. Rawte T, Mavinkurve S (2002) A rapid hypochlorite method for extraction of polyhydroxyalkanoates from bacterial cells. Indian Journal of Experimental Biology, 40(8): 924–929.
25. Mascarenhas J, Aruna K (2017) Screening of polyhydroxyalkanoates (PHA) accumulating bacteria from diverse habitats. Journal of Global Biosciences 6(3): 4835–4848.
26. Williams ST, Sharpe ME, Holt JG (Eds.) (1989) Bergey's Manual of Systematic Bacteriology (Vol. 4). Williams & Wilkins.
27. Marmur J (1961) A procedure for the isolation of deoxyribonucleic acid from micro-organisms. Journal of Molecular Biology 3(2): 208. https://doi.org/10.1016/S0022-2836(61)80047-8
28. Lane DJ (1991) 16S/23S rRNA sequencing. In E Stackebrandt & M Goodfellow (Eds.), Nucleic Acid Techniques in Bacterial Systematics, John Wiley & Sons, pp. 115–175.
29. Altschul SF, Gish W, Miller W, Myers EW, Lipman DJ (1990) Basic local alignment search tool. Journal of Molecular Biology 215(3): 403–410. https://doi.org/10.1016/S0022-2836(05)80360-2
30. Tamura K, Stecher G, Peterson D, Filipski A, Kumar S (2013) MEGA6: Molecular evolutionary genetics analysis version 6.0. Molecular Biology and Evolution 30(12): 2725–2729. https://doi.org/10.1093/molbev/mst197
31. Kumar P, Patel SKS, Lee JK, Kalia VC (2013) Extending the limits of *Bacillus* for novel biotechnological applications. Biotechnology Advances 31(8): 1543–1561. https://doi.org/10.1016/j.biotechadv.2013.08.007
32. Muigano MN, Anami SE, Onguso JM, Mauti GO (2024) Optimized poly(3-hydroxybutyrate-co-3-hydroxyvalerate) (PHBV) production by moderately haloalkaliphilic bacterium *Halomonas alkalicola* Ext. International Journal of Polymer Science 2024: 6667843. https://doi.org/10.1155/2024/6667843

33. Box GEP, Wilson KB (1951) On the experimental attainment of optimum conditions. Journal of the Royal Statistical Society Series B 13: 1-45. https://doi.org/10.1111/j.2517-6161.1951.tb00067.x
34. Bezerra M A, Santelli R E, Oliveira E P, Villar LS, Escaleira L A (2008) Response surface methodology (RSM) as a tool for optimization in analytical chemistry. Talanta 76(5): 965–977. https://doi.org/10.1016/j.talanta.2008.05.019
35. Mohammed S, Ray L (2022) Polyhydroxyalkanoate recovery from newly screened *Bacillus* sp. LPPI-18 using various methods of extraction from Loktak Lake sediment sample. Journal of Genetic Engineering and Biotechnology 20(1): 115. https://doi.org/10.1186/s43141-022-00392-7
36. Law JH, Slepecky RA (1961) Assay of poly-β-hydroxybutyric acid. Journal of Bacteriology 82(1): 33–36. https://doi.org/10.1128/jb.82.1.33-36.1961
37. Pachiyappan S, Dawn SS, Samrot AV (2016) Production, optimization and characterization of poly[R]hydroxyalkanoate from *Enterobacter* sp. SU16. Indian Journal of Science and Technology 9(45): 416-427. https://doi.org/10.1049/iet-nbt.2018.5053
38. Ramadas NV, Singh SK, Soccol CR, Pandey A (2009) Polyhydroxybutyrate production using agro-industrial residue as substrate by *Bacillus sphaericus* NCIM 5149. Brazilian Archives of Biology and Technology 52(1): 17–23. https://doi.org/10.1590/S1516-89132009000100003
39. Rao A, Haque S, El-Enshasy HA, Singh V, Mishra BN (2019) RSM–GA based optimization of bacterial PHA production and in silico modulation of citrate synthase for enhancing PHA production. Biomolecules 9(12): 872. https://doi.org/10.3390/biom9120872
40. Sathya AB, Sivasubramanian V (2015) Screening and molecular characterization of a native isolate *Pseudomonas aeruginosa* NA08 producing polyhydroxyalkanoates. International Journal of Biological Macromolecules 81: 1128–1136. https://doi.org/10.1016/j.ijbiomac.2015.09.048
41. Braunegg G, Sonnleitner B, Lafferty RM (1978) A rapid gas chromatographic method for the determination of poly-β-hydroxybutyric acid in microbial biomass. European Journal of Applied Microbiology and Biotechnology, 6(1): 29–37. https://doi.org/10.1007/BF00500854
42. Yadav B, Wei Y, Pilla S, Tremblay J (2024) Acid hydrolysis of *Solanum tuberosum* periderm for accumulation of polyhydroxyalkanoates in *Pseudomonas putida* MTCC

2475. Frontiers in Bioengineering and Biotechnology, 12: 1343540. https://doi.org/10.3389/fbioe.2024.1343540

43. Lorini L, Martinelli A, Capuani G, Frison N, Reis M, Sommer Ferreira B, Villano M, Majone M, Valentino F (2021) Characterization of polyhydroxyalkanoates produced at pilot scale from different organic wastes. Frontiers in Bioengineering and Biotechnology 9: 628719. https://doi.org/10.3389/fbioe.2021.628719
44. Brinda Devi A, Valli Nachiyar C, Kaviyarasi T, Samrot AV (2015) Characterization of polyhydroxybutyrate synthesized by *Bacillus cereus*. International Journal of Pharmacy and Pharmaceutical Sciences 7(3): 140–144.
45. Mandragutti T, Sudhakar G (2023) Selective isolation and genomic characterization of biopolymer producer—a novel feature of halophile *Brachybacterium paraconglomeratum* MTCC 13074. Journal of Genetic Engineering and Biotechnology 21: 24. https://doi.org/10.1186/s43141-023-00484-y
46. Nwinyi OC, Owolabi TA (2019) Scanning electron microscopy and Fourier transmission analysis of polyhydroxyalkanoates isolated from bacterial species from Abattoir in Ota, Nigeria. Journal of King Saud University – Science 31(3): 285–298. https://doi.org/10.1016/j.jksus.2017.08.003
47. Phanse N, Chincholikar A, Patel B, Rathore P, Vyas P, Patel M (2011) Screening of PHA (polyhydroxyalkanoate) producing bacteria from diverse sources. International Journal of Biosciences 1(6): 27–32.
48. Ostle AG, Holt JG (1982) Nile blue A as a fluorescent stain for poly-β-hydroxybutyrate. Applied and Environmental Microbiology 44(1): 238–241. https://doi.org/10.1128/aem.44.1.238-241.1982
49. Suguna PP, Saranya VV, Abirami PP, Shenbagarathai RR (2020) Optimization and characterization of PHA (SCL-SCL) copolymer by indigenous *Bacillus thuringiensis* A102 strain for biomedical applications. Current Microbiology 77: 3978–3989. https://doi.org/10.1007/s00284-020-02221-x
50. Singh S, Sithole B, Lekha P, Permaul K, Govinden R (2021) Optimization of cultivation medium and cyclic fed-batch fermentation strategy for enhanced polyhydroxyalkanoate production by *Bacillus thuringiensis* using a glucose-rich hydrolyzate. Bioresources and Bioprocessing 8: 1–17. https://doi.org/10.1186/s40643-021-00361-x
51. Cueva-Almendras LC, Alvarado JCA, Fuentes-Olivera AJ, Llontop-Bernabe KS, Cerna CEQ, Rodriguez-Soto JC, Cruz-Monzon JA, Alvarez MAQ (2022) Production

of polyhydroxyalkanoate by *Bacillus thuringiensis* isolated from agricultural soils of Cascas-Peru. Brazilian Archives of Biology and Technology 65: e22220107 https://doi.org/10.1590/1678-4324-2022220107

52. El-Sheekh MM, El-Abd MA, El-Diwany AI, Ismail AMS, Omar TH (2015) Poly-3-hydroxybutyrate (PHB) production by *Bacillus flexus* ME-77 using some industrial wastes. Rendiconti Lincei 26: 109–119. https://doi.org/10.1007/s12210-014-0368-z
53. Thapa C, Shakya P, Shrestha R, Pal S., Manandhar P (2018) Isolation of polyhydroxybutyrate (PHB) producing bacteria, optimization of culture conditions for PHB production, extraction and characterization of PHB. Nepal Journal of Biotechnology 6(1): 62–68.
54. Ponnusamy S, Viswanathan S, Periyasamy A, Rajaiah S (2019) Production and characterization of PHB-HV copolymer by *Bacillus thuringiensis* isolated from *Eisenia foetida*. Biotechnology and Applied Biochemistry, 66(3): 340–352. https://doi.org/10.1002/bab.1730
55. Narayanan M, Kandasamy G, Murali P, Kandasamy S, Ashokkumar V, Nasif O, Pugazhendhi A (2021) Optimization and production of polyhydroxybutyrate from sludge by *Bacillus cereus* categorized through FT-IR and NMR analyses. Journal of Environmental Chemical Engineering, 9(1): 104908. https://doi.org/10.1016/j.jece.2020.104908
56. Mohanrasu K, Rao RGR, Dinesh GH, Zhang K, Prakash GS, Song DP, Muniyasamy S, Pugazhendhi A, Jeyakanthan J, Arun, A (2020) Optimization of media components and culture conditions for polyhydroxyalkanoates production by *Bacillus megaterium*. Fuel, 271: 117522. https://doi.org/10.1016/j.fuel.2020.117522
57. Zihayat B, Shakibaie M, Sabouri-Shahrbabak S, Doostmohammadi M, Ameri A, Adeli-Sardou M, Forootanfar H (2019) Medium optimization for polyhydroxyalkanoate production by *Pseudomonas pseudoalcaligenes* strain Te using D-optimal design. Biocatalysis and Agricultural Biotechnology, 18: 101001. https://doi.org/10.1016/j.bcab.2019.01.039
58. Sachan RSK, Kumar A, Karnwal A, Paramasivam P, Agrawal A, Ayanie AG (2025) Screening and characterization of PHA-producing bacteria from sewage water identifying *Bacillus paranthracis* RSKS-3 for bioplastic production. BMC Microbiology 25: 136. https://doi.org/10.1186/s12866-025-03841-8
59. Ibrahim MI, Esmael ME, Elmashi TR, Haga T, Bayoumi RA, Eldanasoury MM, Sofy MR, Matsuo K, Khattab AM (2024) Structure assessment and impacts of lipids'

chemistry on the structuration of polyhydroxyalkanoate biosynthesized by *Bacillus licheniformis* AZU-A5. Chirality 36(10): e23722. https://doi.org/10.1002/chir.23722

60. Sachan RSK, Devgon I, Al-Tawaha ARMS, Karnwal A (2024) Optimizing polyhydroxyalkanoate production using a novel *Bacillus paranthracis* isolate: A response surface methodology approach. Heliyon, 10(15): e35398. https://doi.org/10.1016/j.heliyon.2024.e35398
61. Semeniuk I, Pokynbroda T, Kochubei V, Midyana H, Karpenko O, Skorokhoda V (2020) Biosynthesis and characteristics of polyhydroxyalkanoates. 1. polyhydroxybutyrates of *Azotobacter vinelandii* n-15. Chemistry & Chemical Technology 14(4): 463–467. https://doi.org/10.23939/chcht14.04.463
62. Gedikli S, Celik PA, Demirbilek M, Mutlu MB, Denkbaş EB, Cabuk A (2019) Experimental exploration of thermostable poly(β-hydroxybutyrates) by *Geobacillus kaustophilus* using Box-Behnken design. Journal of Polymers and the Environment 27: 245–255. https://doi.org/10.1007/s10924-018-1335-z
63. Stanley A, Murthy PK, Vijayendra SVN (2020) Characterization of polyhydroxyalkanoate produced by *Halomonas venusta* KT832796. Journal of Polymers and the Environment 28: 973–983. https://doi.org/10.1007/s10924-020-01662-6
64. Sedlacek P, Slaninova E, Enev V, Koller M, Nebesarova J, Marova I, Hrubanova K, Krzyzanek V, Samek O Obruca S (2019) What keeps polyhydroxyalkanoates in bacterial cells amorphous? A derivation from stress exposure experiments. Applied Microbiology and Biotechnology 103(4): 1905–1917. https://doi.org/10.1007/s00253-018-09584-z
65. Lee HJ, Kim SG, Cho DH, Bhatia SK, Gurav R, Yang SY, Yang J, Jeon JM, Yoon JJ, Choi KY, Yang YH (2022) Finding of novel lactate utilizing *Bacillus* sp. YHY22 and its evaluation for polyhydroxybutyrate (PHB) production. International Journal of Biological Macromolecules 201: 653–661. https://doi.org/10.1016/j.ijbiomac.2022.01.025
66. Barnard GN, Sanders JK (1989) The poly-β-hydroxybutyrate granule in vivo: a new insight based on NMR spectroscopy of whole cells. Journal of Biological Chemistry 264(6): 3286-3291.
67. Jendrossek D (2009) Polyhydroxyalkanoate granules are complex subcellular organelles (carbonosomes). Journal of Bacteriology 191(10): 3195-3202. https://doi.org/10.1128/jb.01723-08

68. Sudesh K, Abe H, Doi Y (2000) Synthesis, structure and properties of polyhydroxyalkanoates: biological polyesters. Progress in Polymer Science 25(10): 1503-1555. https://doi.org/10.1016/S0079-6700(00)00035-6
69. Jacquel N, Lo CW, Wei YH, Wu HS, Wang SS (2008) Isolation and purification of bacterial poly (3-hydroxyalkanoates). Biochemical Engineering Journal 39(1): 15-27. https://doi.org/10.1016/j.bej.2007.11.029
70. Barham PJ, Keller A, Otun EL, Holmes PA (1984) Crystallization and morphology of a bacterial thermoplastic: poly-3-hydroxybutyrate. Journal of Materials Science 19(9): 2781-2794. https://doi.org/10.1007/BF01026954
71. Singh M, Patel SK, Kalia VC (2009) *Bacillus subtilis* as potential producer for polyhydroxyalkanoates. Microbial Cell Factories 8(1): 38. https://doi.org/10.1186/1475-2859-8-38
72. Valappil SP, Peiris D, Langley GJ, Herniman JM, Boccaccini AR, Bucke C, Roy I (2007) Polyhydroxyalkanoate (PHA) biosynthesis from structurally unrelated carbon sources by a newly characterized Bacillus spp. Journal of Biotechnology 127(3): 475-487. https://doi.org/10.1016/j.jbiotec.2006.07.015
73. Jendrossek D, Handrick R (2002) Microbial degradation of polyhydroxyalkanoates. Annual Review of Microbiology 56(1): 403-432. https://doi.org/10.1146/annurev.micro.56.012302.160838
74. Anderson AJ, Dawes EA (1990) Occurrence, metabolism, metabolic role, and industrial uses of bacterial polyhydroxyalkanoates. Microbiological Reviews 54(4): 450-472. https://doi.org/10.1128/mr.54.4.450-472.1990
75. Lee SY (1996) Bacterial polyhydroxyalkanoates. Biotechnology and Bioengineering, 49(1): 1-14. https://doi.org/10.1002/(SICI)1097-0290

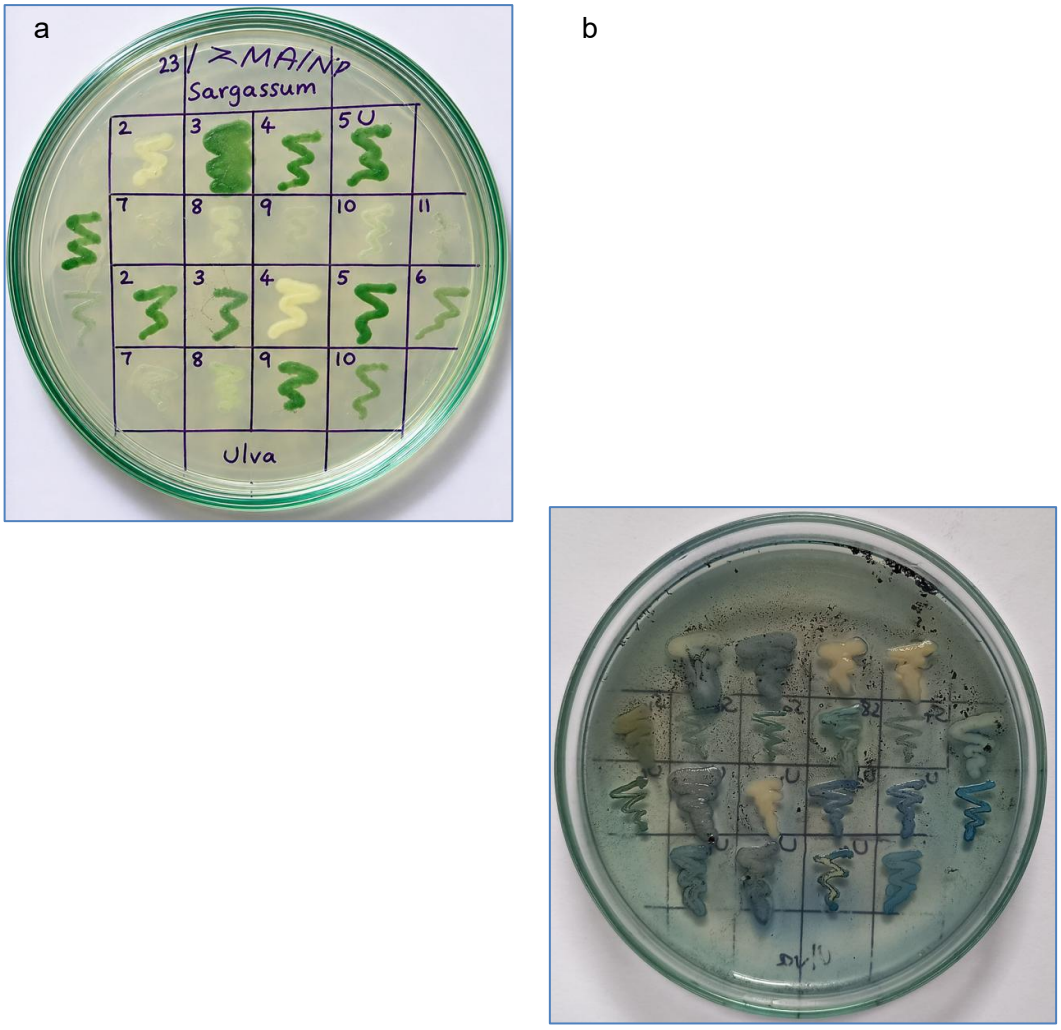


Fig. 1 Sudan black B staining of the isolated seaweed-associated bacterial strains (a-Back side view, b-Front side view)



Fig. 2 Nile blue-A staining of the bacterial strains which isolated from seaweed association

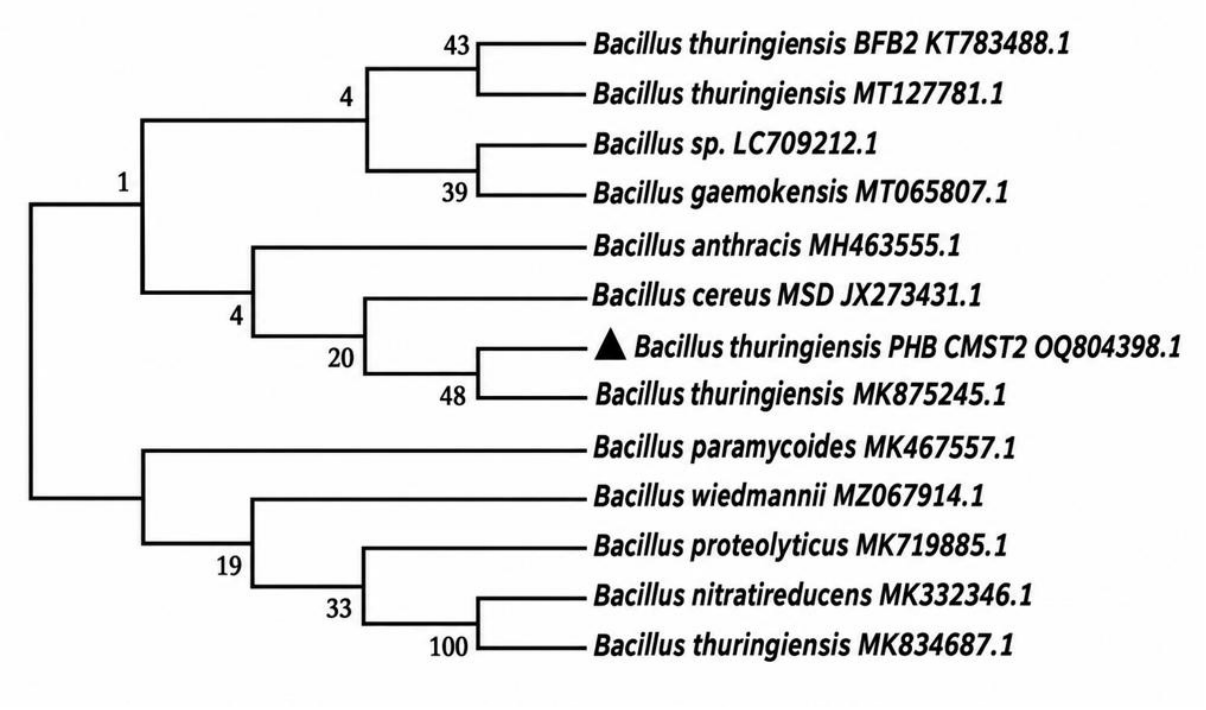


Fig. 3 Phylogenetic relationship based on 16S rRNA of the bacterial strain S4 *Bacillus thuringiensis* PHB CMST2

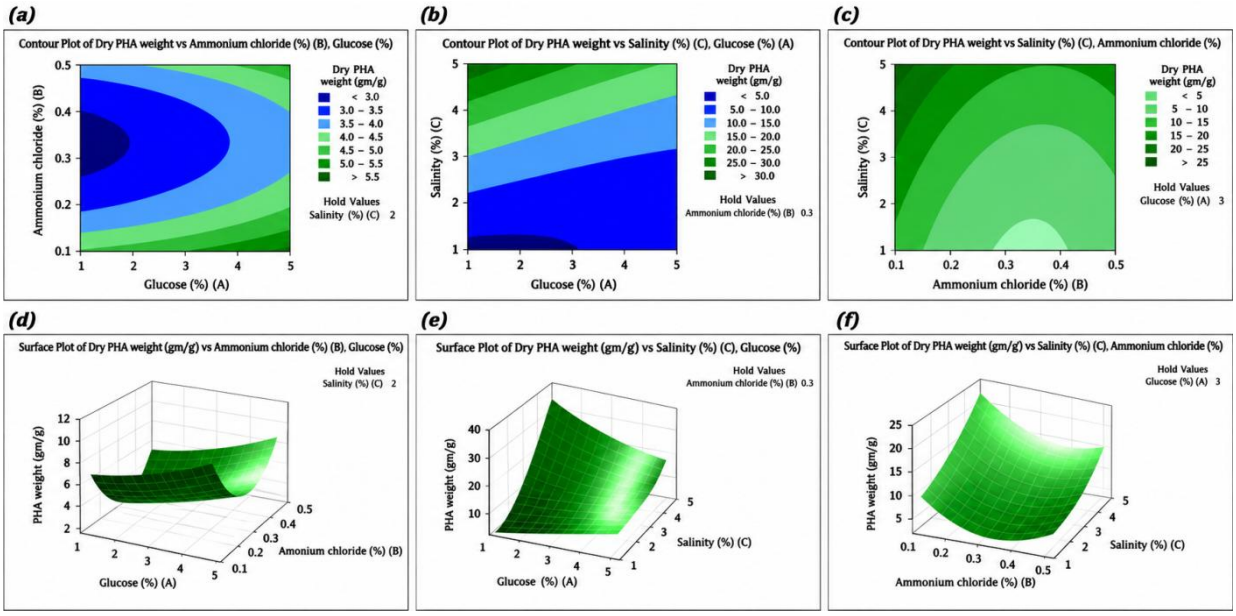


Fig. 4 Three-dimensional response surfaces and contour plots of the effect of glucose, ammonium chloride, and salinity on PHA production in *B. thuringiensis* strain PHB CMST2

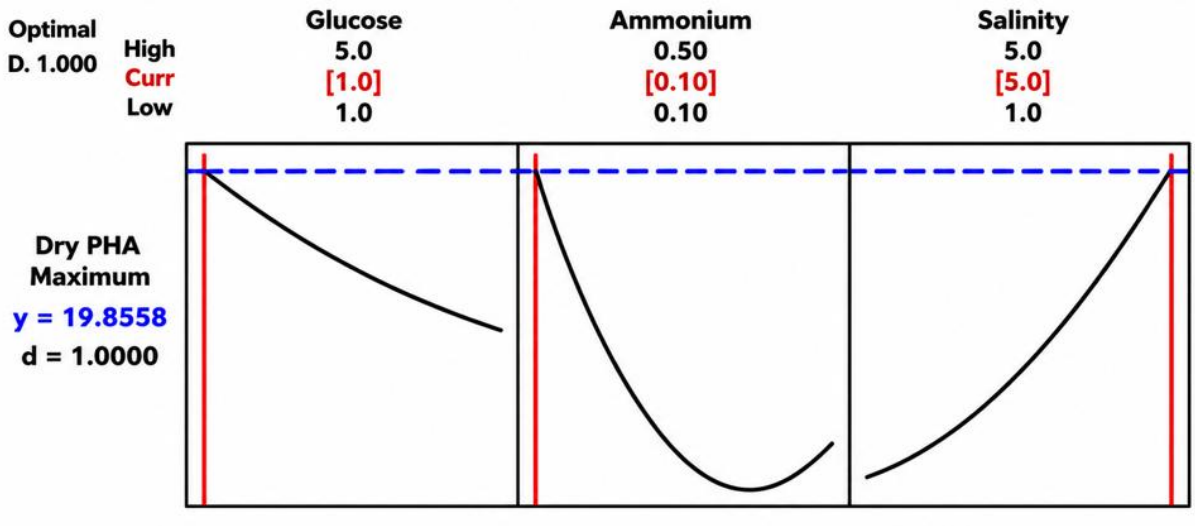


Fig. 5 Numerical optimization of the fitted model for maximum PHA production in *B. thuringiensis* strain PHB CMST2



Fig. 6 PHA biofilm from the *B. thuringiensis* strain PHB CMST2

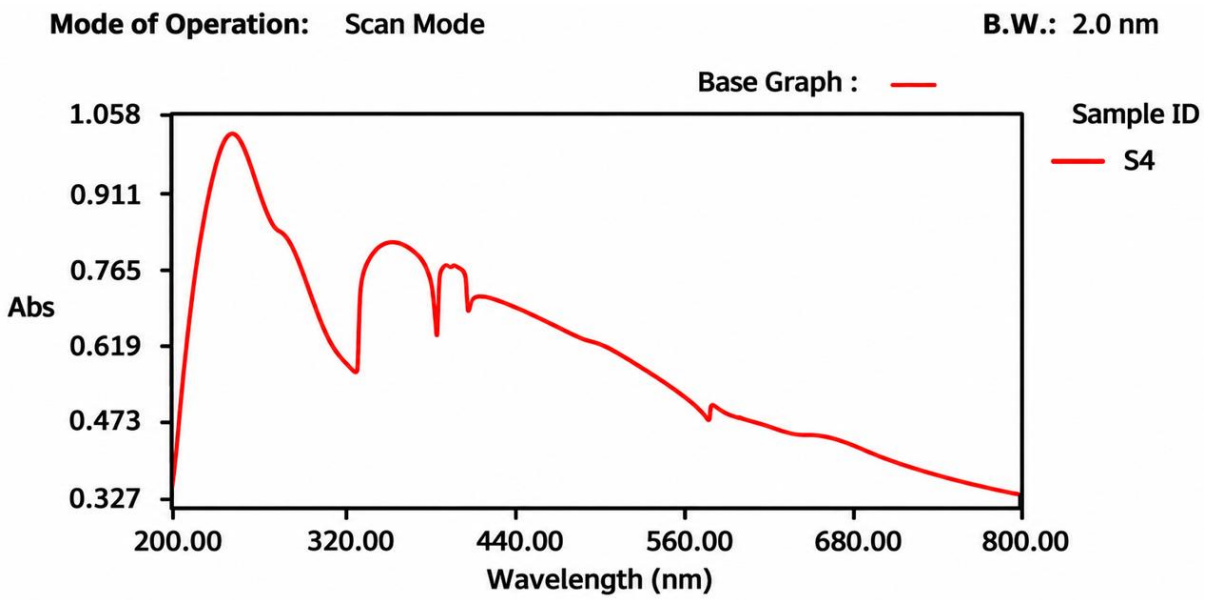


Fig. 7 UV-visible spectral analysis of the extracted PHA in *B. thuringiensis* strain PHB CMST2



Fig. 8 TLC plate showing the presence of PHA in *B. thuringiensis* strain PHB CMST2

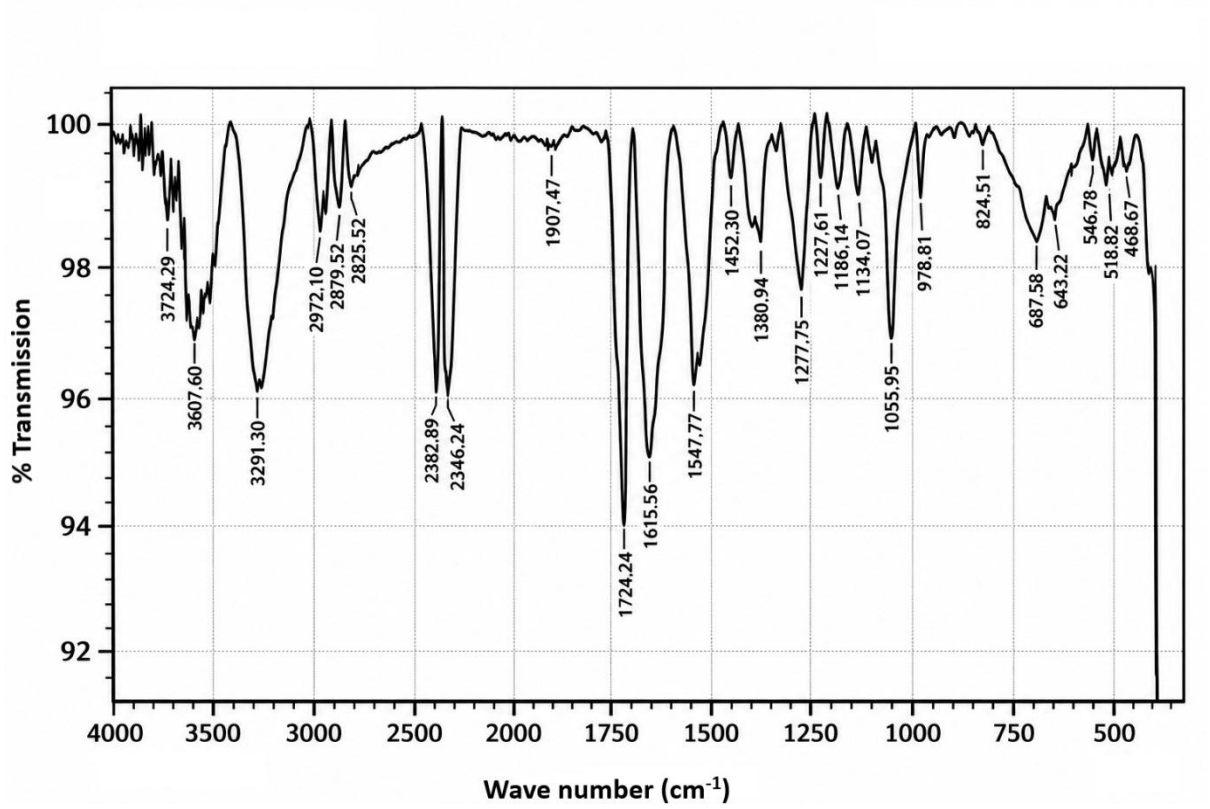


Fig. 9 Fourier-transform infrared (FT-IR) spectra of extracted PHA from *B. thuringiensis* strain PHB CMST2

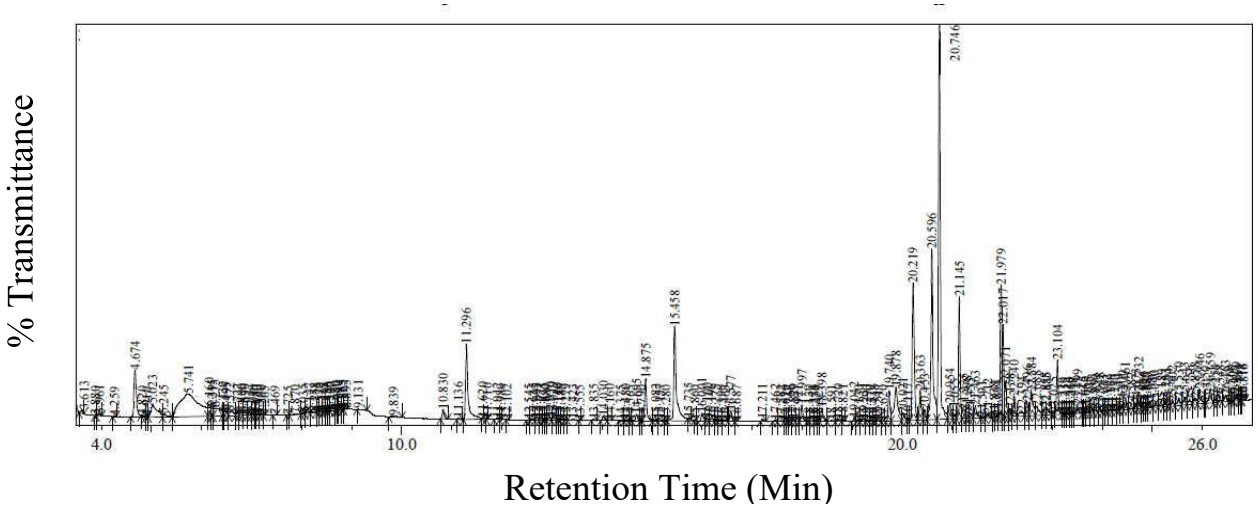


Fig. 10 GC-MS analysis of the extracted PHA from *B. thuringiensis* strain PHB CMST2

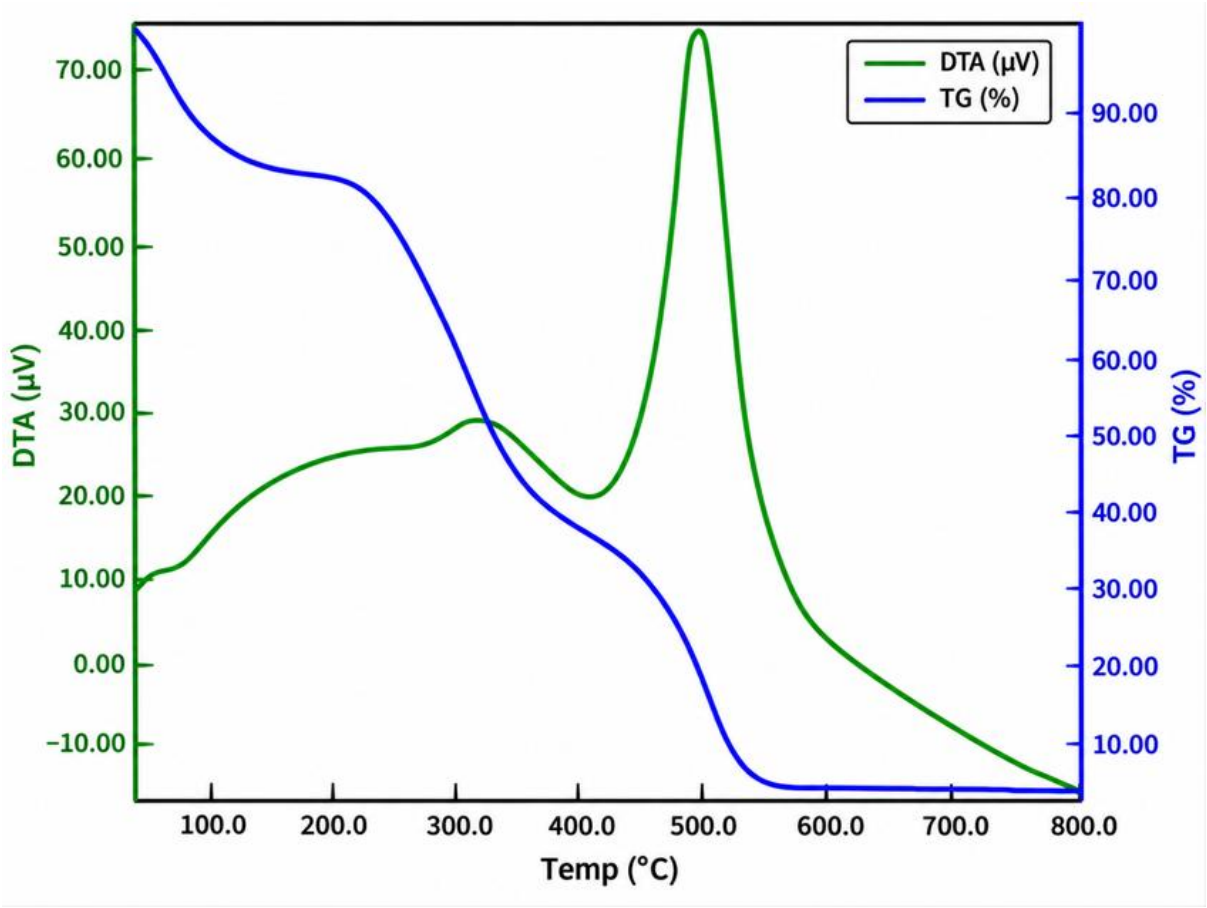


Fig. 11 Thermogravimetric analysis of the extracted PHA from *B. thuringiensis* strain PHB CMST2

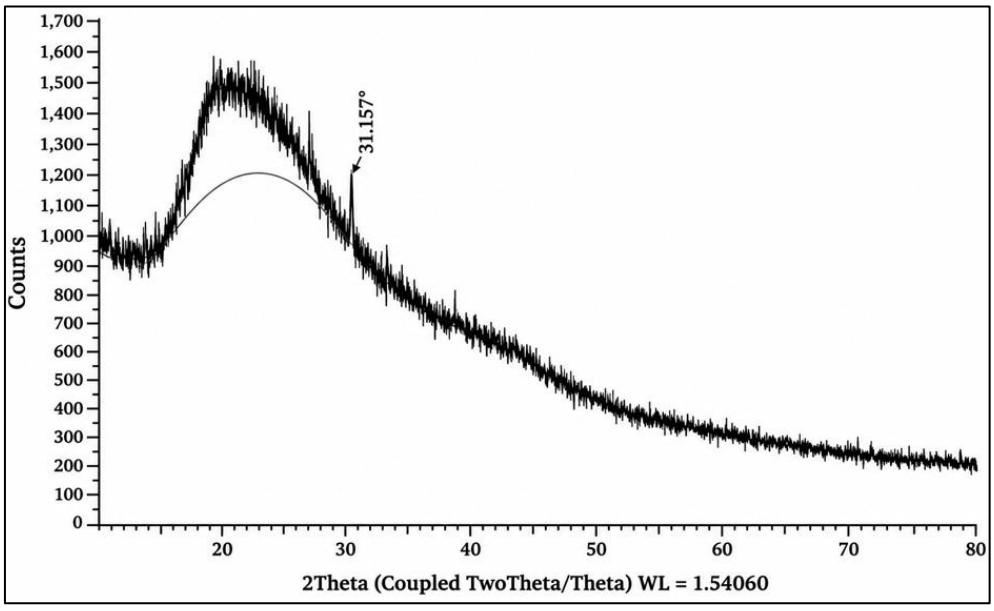


Fig. 12 X-ray diffractogram of the extracted PHA from *B. thuringiensis* strain PHB CMST2

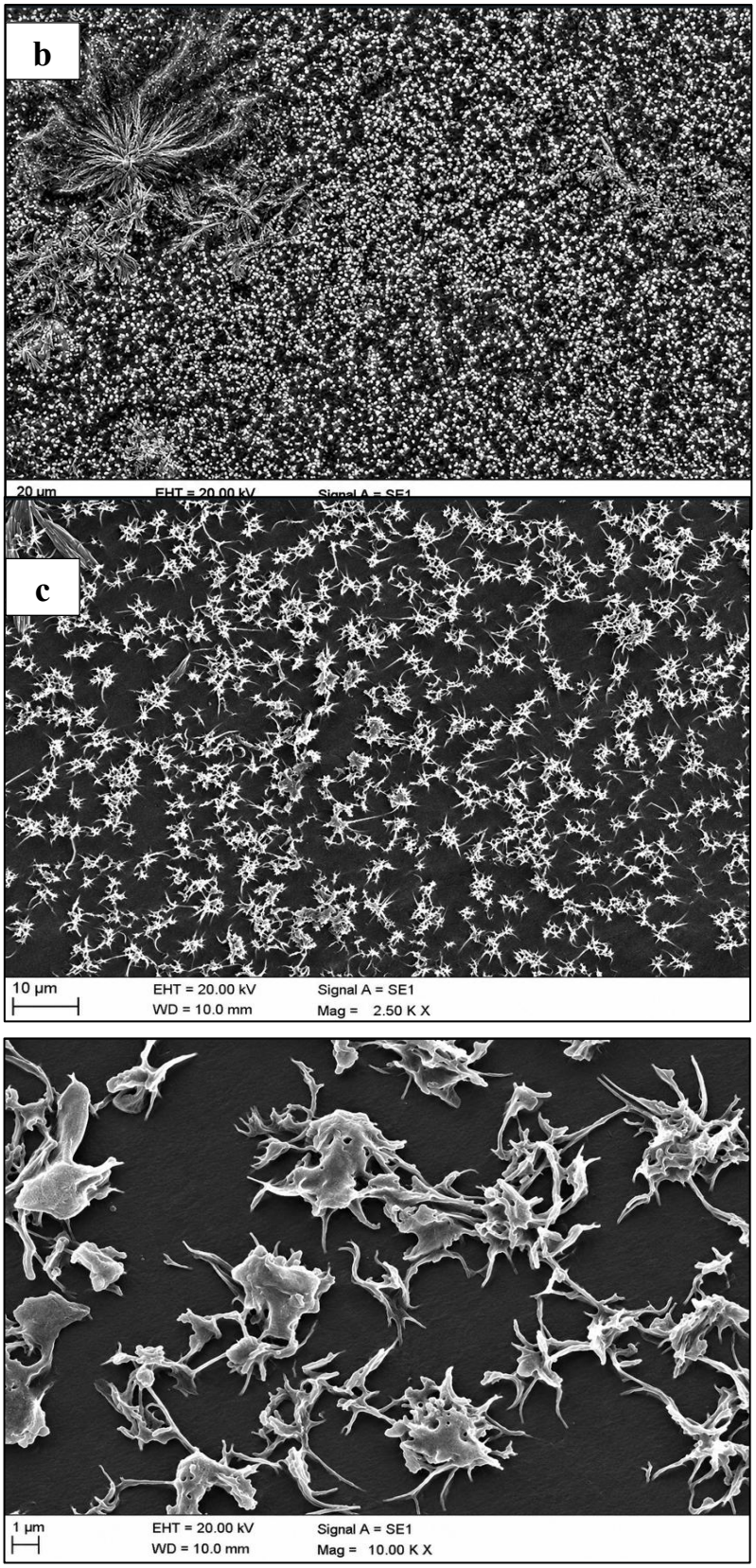


Fig. 13 SEM micrographs of extracted PHA from *Bacillus thuringiensis* strain PHB CMST2 at (a) 500×, (b) 2,500× and (c) 10,000×

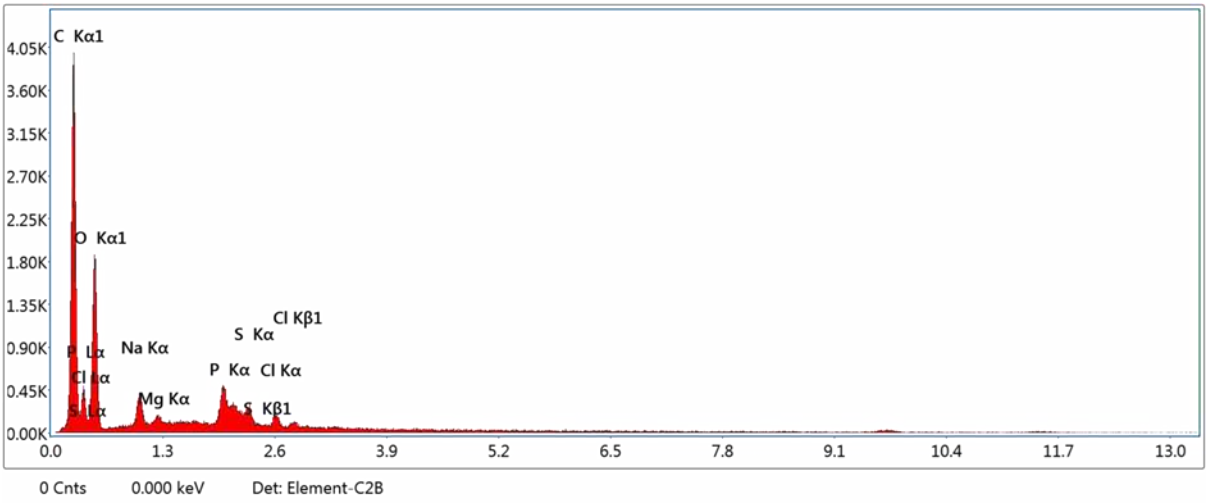


Fig. 14 Elemental mapping of the extracted PHA from *B. thuringiensis* strain PHB CMST2